Transactions, **SMiRT-25**
Charlotte, NC, USA, August 4-9, 2019
Division VII (Safety, Reliability, Risk and Safety Margins), Paper ID 718

NONLINEAR FINITE ELEMENT ANALYSIS OF SEISMIC LOADS ON RPV INTERNALS

Roland Hilpert[1], Eugen Fütterer[2], Johannes Schmidl[3], Manuel Pellissetti[4], Sunay Stäuble-Akcay[5] and Andrii Nykyforchyn[6]

[1] FRAMATOME GmbH, Erlangen, Germany, (roland.hilpert@framatome.com)
[2] FRAMATOME GmbH, Erlangen, Germany, (eugen.fuetterer@framatome.com)
[3] FRAMATOME GmbH, Erlangen, Germany, (johannes.schmidl@framatome.com)
[4] FRAMATOME GmbH, Erlangen, Germany, (manuel.pellissetti@framatome.com)
[5] Gösgen-Däniken Nuclear Power Plant, Switzerland, (sstaeuble@kkg.ch)
[6] Gösgen-Däniken Nuclear Power Plant, Switzerland, (anykyforchyn@kkg.ch)

ABSTRACT

The paper presents analytical results for the dynamic analysis of the control rod drive mechanisms (CRDM) and selected Reactor Pressure Vessel (RPV) internals, i.e. core barrel (CB) upper flange and upper core plate centering, as well as resulting stresses. The model for the dynamic analysis of the RPV Internals with CESHOCK consists of springs and lumped masses, combined with beam elements (cp. Figure 1).

The model is taking into account material nonlinearities, sliding, friction and gap/impact effects inside the RPV. Refined finite element modelling of contact regions is used to calibrate the force-displacement relationship used in the dynamic model (cp. Figure 2).

Both deterministic and probabilistic analyses are presented. The excitations are based on upstream TH analyses with a coupled model of the nuclear steam supply system (NSSS) and the reactor building, Rangelow et.al. (2017). Variability of soil parameters (shear modulus and damping) and building parameters (Young's modulus and damping) is taken into account. Besides providing the basis for stress analysis of the RPV internals, the dynamic analysis provides excitations at the lower core support, the upper core plate and the middle of the spacer grid level for dedicated nonlinear fuel assembly analyses.

INTRODUCTION

In response to the requirements by the Swiss nuclear regulator (ENSI) Gösgen Nuclear Power Plant (KKG) is performing a seismic re-evaluation of the NSSS including the RPV internals. The purpose of the presented analysis is to determine the seismic loads on the CRDM, the fuel assemblies (FA) and the RPV internals, as the updated seismic hazard level "ENSI-2015" is significantly exceeding the seismic design loads at the time of commissioning.

MODELLING

The response to seismic-induced excitation is analyzed with a two-dimensional model of the RPV-internals with the CRDM in fully withdrawn position. The complete model is shown in Figure 1. The model has been used in the analyses presented in Pellissetti et.al. (2015), but has not been described in detail in that reference.

Distinct models are used to analyze the responses to horizontal and vertical excitations. The following description refers to the horizontal model. The response to vertical excitations is discussed in a later section of the paper.

The model consists of beams and lumped mass elements as well as linear and nonlinear springs and it takes friction and hydrodynamic coupling into account. It combines the RPV itself with the CB, the FA and the CRDM. The CRDM are grouped in two different sections due to their different length and position on the RPV head. Also the Fuel assemblies (FA) are modelled in 5 groups. The FA can interact with each other and the CB through the springs (representing the spacer grids) and are supported by the upper and lower core plate. Between the RPV and the CB the fluid is modelled via a hydrodynamic coupling. This introduces non zero values into the mass matrix outside of the diagonal. The masses of the individual components are evaluated in detail, including the mass moments of inertia, and applied as lumped masses (mass moments of inertia) to the model.

On the right of Figure 1 (at node 12, red box) the anchorage of the model to the building is shown. This is the elevation of the support brackets of the RPV. At this node the time histories (TH) from the coupled building-NSSS model (Rangelow et.al. (2017)) are applied as excitation.

The horizontal model also accounts for the rocking motion of the RPV. Thus, the excitation at node 12 consists of both the translation in one horizontal direction and the rotation around the other horizontal direction.

The motions at the core barrel, the lower support plate, the spacer grid and the upper support plate are used as excitations for subsequent detailed fuel assembly analysis.

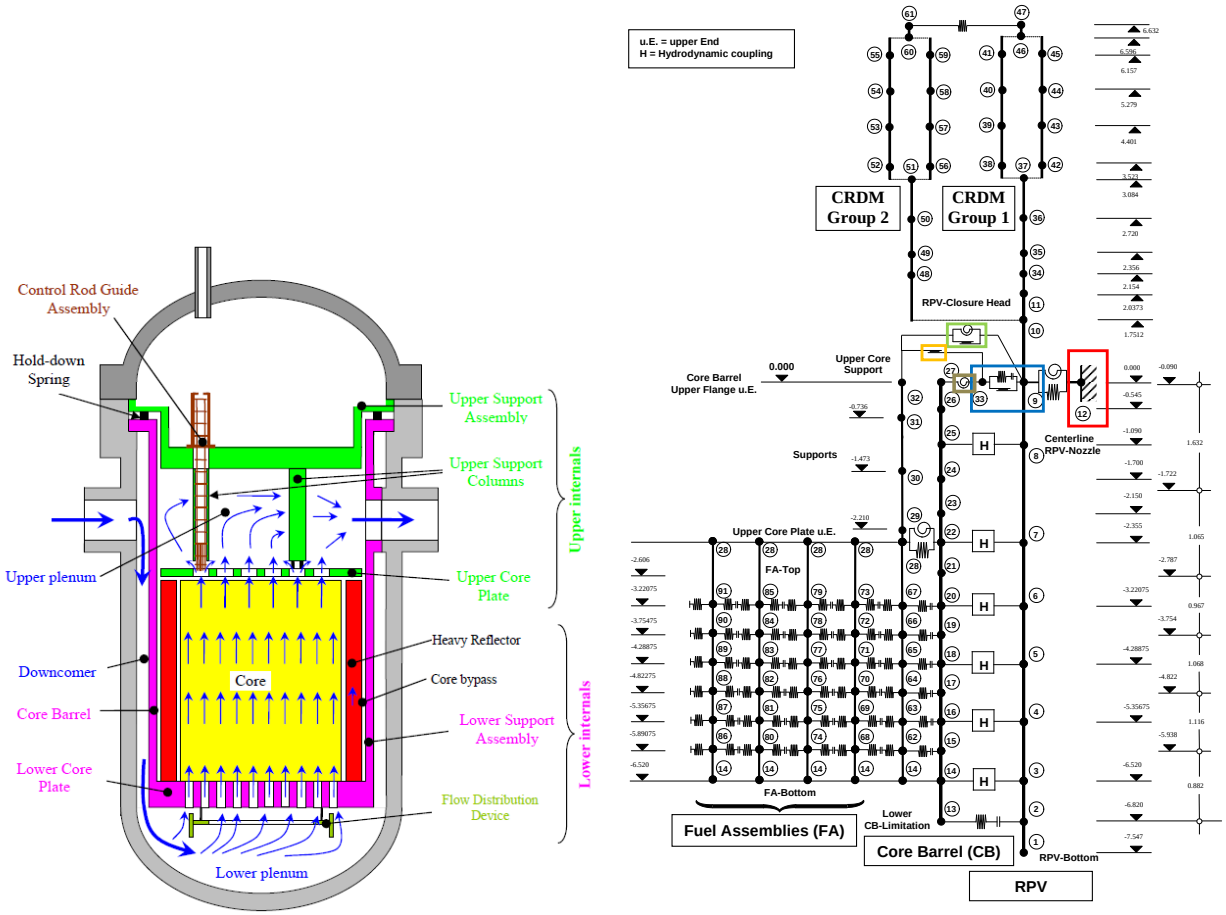

Figure 1. RPV Internals schematic (left) and analysis model for horizontal excitation (right)

Detailed finite element models of contact areas are used to determine the corresponding non-linear force-displacement curves, as shown in Figure 2 for the RPV CB flange alignment. The elasto-plastic stress-strain curves of the different materials (austenitic material for the CB flange with alignment and the cladding of the RPV, ferritic material for the RPV and Inconel for the guidance block) are considered as well as a pre-stress on the flange. Contact areas are modeled by friction elements. On this detailed model a tangential displacement is applied and a resulting tangential reaction is calculated. The resulting non-linear force-displacement curve is applied to the corresponding coupling element of the dynamic analysis model (between node 9 and 33, blue box in Figure 1).

For the other nonlinear connections similar assumptions are applied to consider their corresponding behavior:

- Node 27-33 (brown box): A nonlinear rotational spring of the upper CB flange due to elasto-plastic material behavior is considered
- Node 32-33 (orange box): A frictional connection between the flange of the upper core support and the upper CB flange is introduced
- Node 32-9 (green box): A frictional connection between the flange of the upper core support and the RPV is applied, as well as a stiff rotational spring

Linear lateral springs model the interaction between the FA and the CB, as well as between the CRDM.

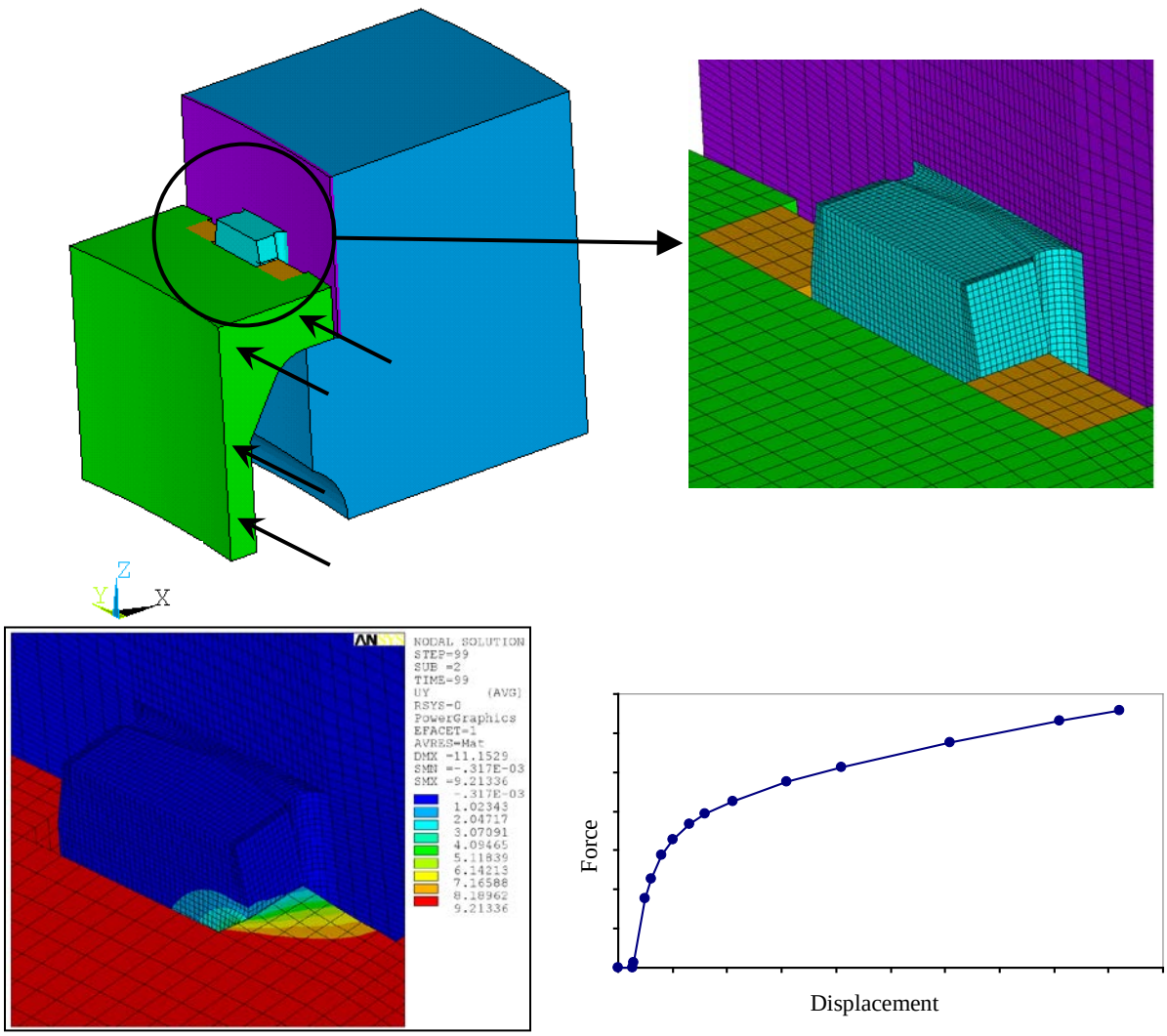

Figure 2. Finite element model of CB flange alignment (Top), Displacement result UY (lower left) and nonlinear force-displacement curve (lower right)

To determine the damping characteristic for the calculation, namely the α and β constants for the Rayleigh damping, the model of Figure 1 is linearized and a modal calculation is performed with ANSYS. Out of these results the damping characteristic of the different eigenmodes are extracted. Some modal results, eigenfrequencies and eigenmodes are shown in Figure 3. The first eigenmode of the FA, the first eigenmode of the CRDM, as well as the second and third eigenmode of the FA for one specific core configuration are shown. Out of these results the lower and upper bound frequencies are extracted and the mass proportional α value and the stiffness proportional β value are calculated.

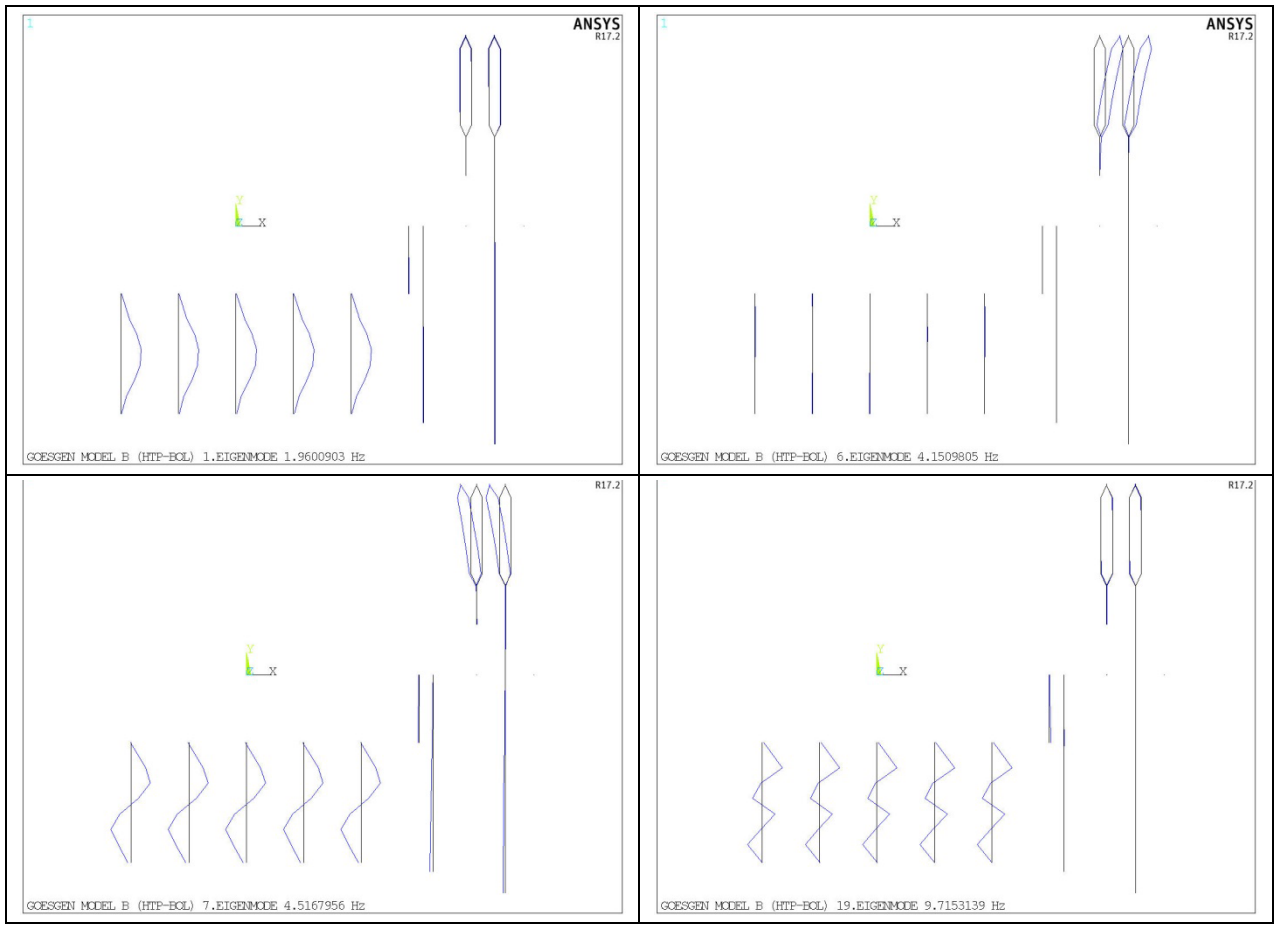

Figure 3. Modal results for some eigenmodes

NONLINEAR TIME HISTORY ANALYSIS (HORIZONTAL MODEL)

Three different types of core configurations (B, E and F) are examined for both the deterministic and the probabilistic analysis. For the deterministic calculation the overall number of calculations is shown in Table 1. Three different soil conditions denoted as w ("weich" → soft), m (medium), s (stiff) are considered and evaluated. For each of them a set of 7 time histories are calculated. The excitations in X (together with the rotation in Y (rotY)) and Y (together with the rotation in X (rotX)) direction are analyzed independently and subsequently combined with the results for the vertical direction (Z).

Table 1: Deterministic calculations

3	**x**	**2**	**x**	**3**	**x**	**7**	**=**	**126**
Core Models (B, E, F)		*Directions (X rotY, Y rotX)*		*Ground Soil Stiffness (m, s, w)*		*Time Histories (TH) (ZV1 – ZV7)*		

For the probabilistic analysis the overall number of calculations is shown in Table 2. Also the two different directions X and Y are calculated independently and a set of 30 time histories is evaluated, so that a total of 180 calculations are performed.

Table 2: Probabilistic calculations

3	**x**	**2**	**x**	**30**	**=**	**180**
Core Models (B, E, F)		*Directions (X rotY, Y rotX)*		*Time Histories (TH) (ZV1 – ZV30)*		

In Figure 4 the displacement and acceleration TH (translation in Y and rotation around X) are shown for TH6. The TH have a non-zero initial value and are corrected to avoid numerical issues.

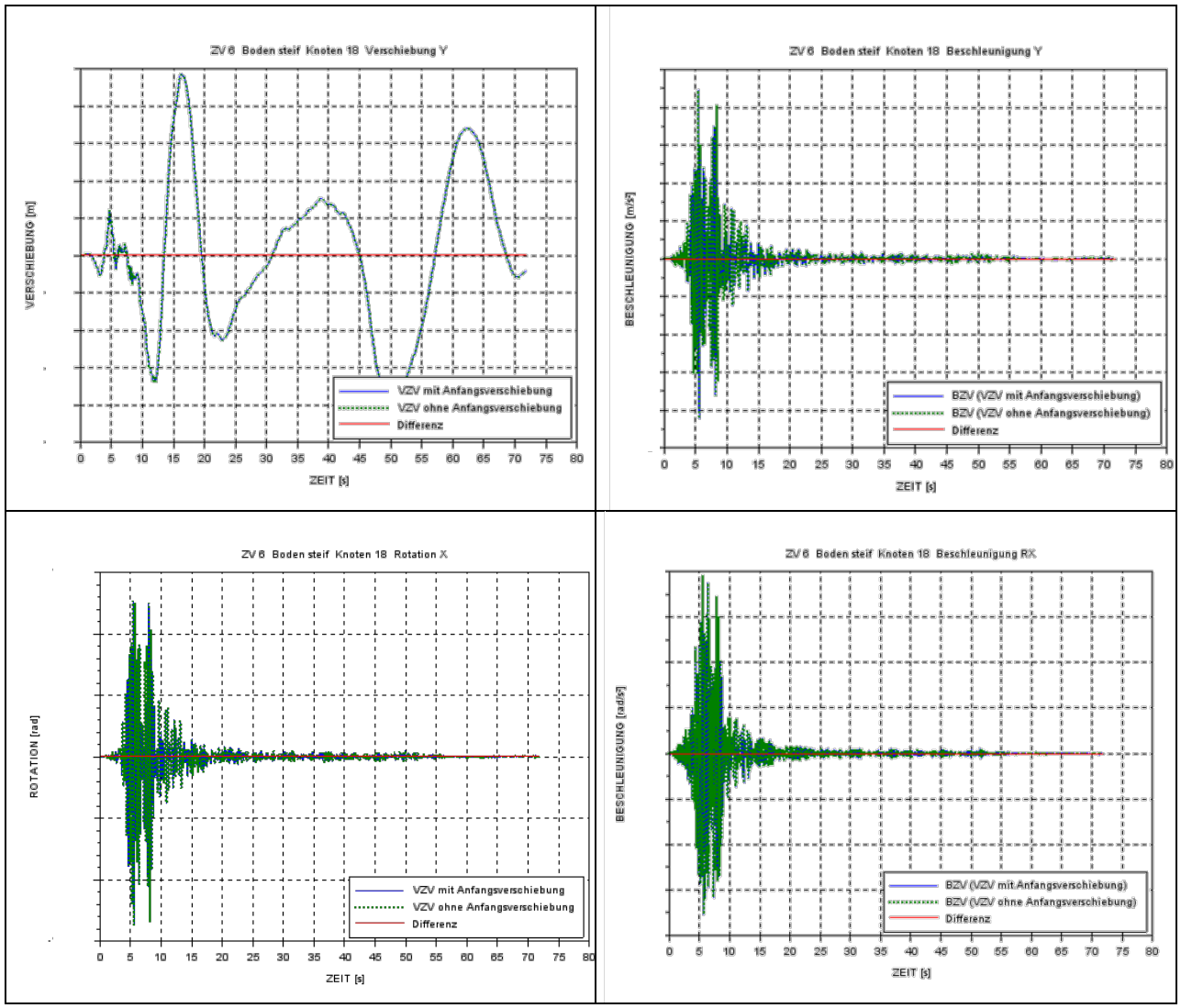

Figure 4. Displacement and acceleration TH (translation Y and rotation around X) for TH6, stiff soil

The acceleration response spectra corresponding to the deterministic and the probabilistic sets of TH are shown in Figure 5 and Figure 6, respectively. The response spectra correspond to node 18, in the proximity of the RPV support, horizontal direction X (the results for direction Y are similar).

The envelopes of the deterministic and the probabilistic spectra are similar. For the probabilistic spectra the second peak is somewhat higher.

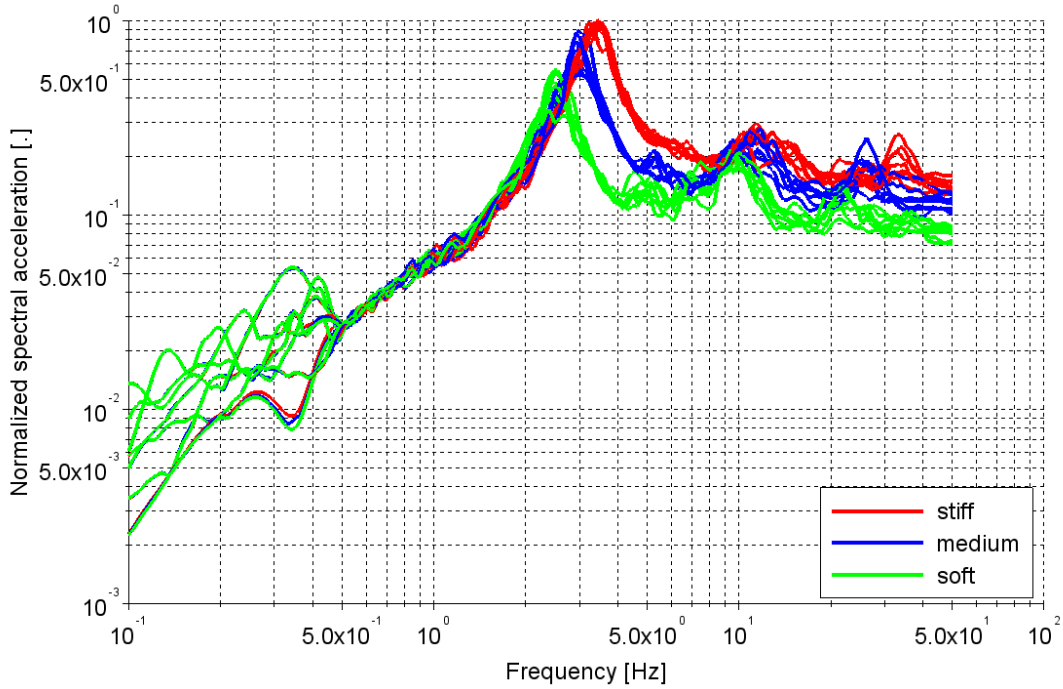

Figure 5. Deterministic acceleration response spectra, 4% damping, X direction at node 18

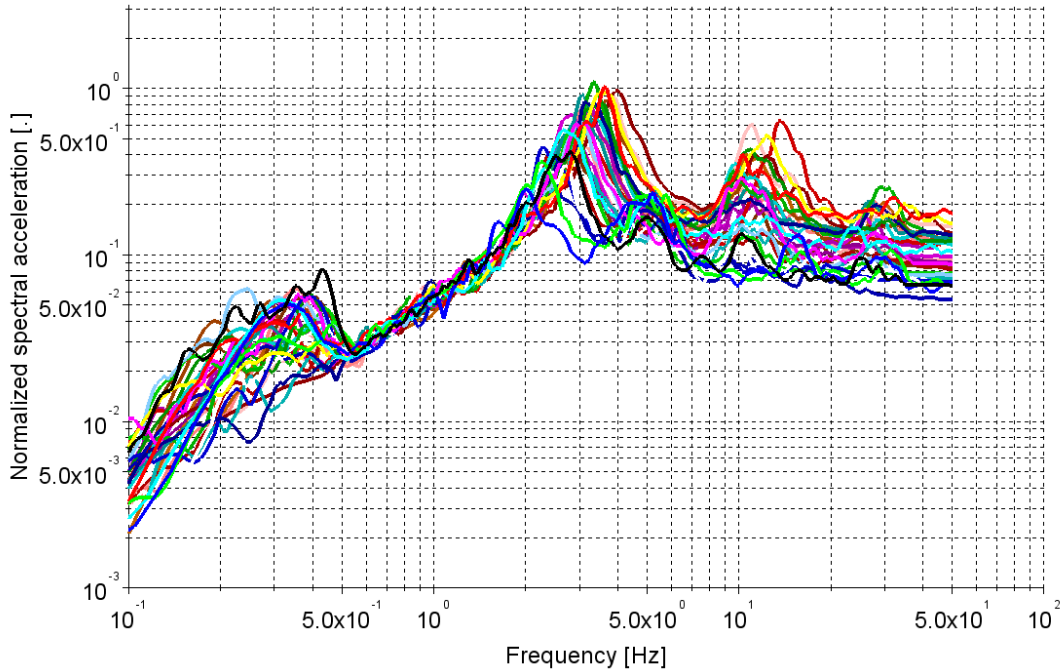

Figure 6. Probabilistic acceleration response spectra, 4% damping, X direction at node 18

For some time histories an accumulation of relative displacement between the upper core support and upper CB flange (cp. Figure 7) is observed. Rather than stepwise sliding, the behavior can be characterized as a slow drift starting in the later phase of the TH. The observed phenomenon is associated with the long duration of some of the time histories.

Due to this observation the model of Figure 1 is extended with a lateral gap element and a stiff spring for a closed gap between the connection of the nodes 32 and 33 (connection between the flange of the upper core support and the upper CB flange, orange box). The impact is modelled as a hard impact as it is assumed that this leads to maximum impact forces. However, since the drift is a slow process the overall effect is low and the forces / stresses are not significantly increased.

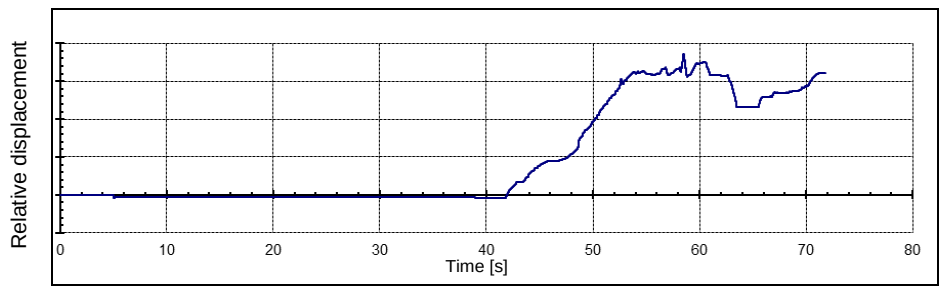

Figure 7. TH6 - relative displacement between upper CB flange and upper core support Model E, stiff soil

SCALING OF RESPONSE TO VERTICAL EXCITATIONS

The loads resulting from the vertical excitations are estimated by scaling the results obtained with the vertical model for the seismic design excitation. The scaling factor is determined through comparison of the new spectra with the design spectra at the relevant vertical frequencies. This comparison and the relevant frequencies are shown in Figure 8. The loads associated with the horizontal and the vertical excitation, respectively, are combined in the subsequent strength analysis.

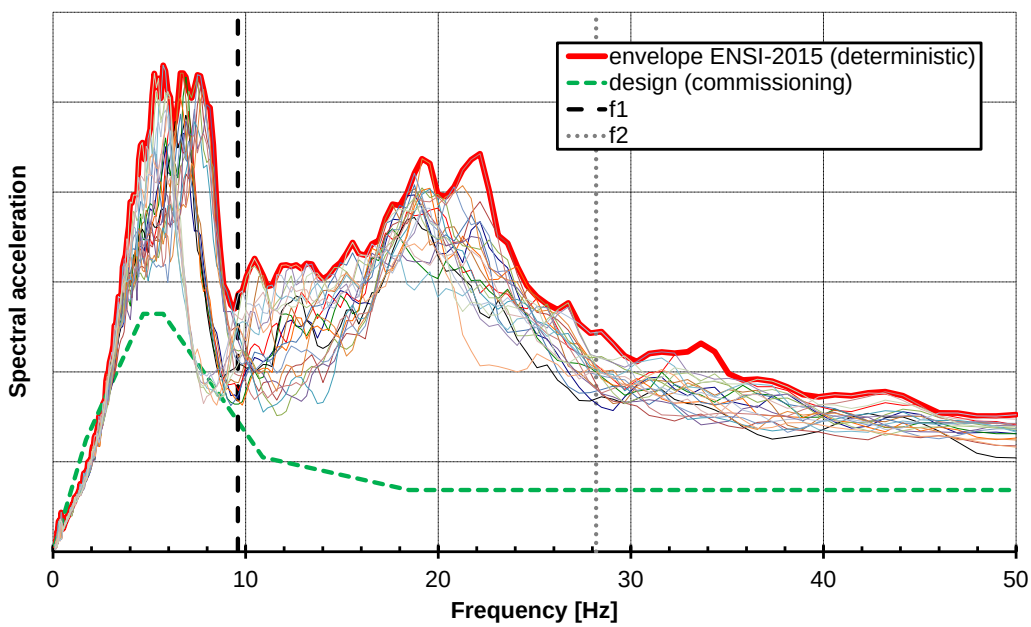

Figure 8. Acceleration Spectra for design spectra and ENSI-2015 loads in vertical direction

STRESS RESULTS

The maximum membrane and bending stresses due to the TH calculations for the CB flange and the CRDM pressure housing are calculated. For the CRDM pressure housing the stresses are evaluated in three different areas: 1. lower pressure housing, thick part, 2. lower pressure housing, thin part, 3. upper pressure housing. The stresses are set into relationship with their corresponding allowable stress and the stress ratios are evaluated. These normalized stress ratios are shown in Figure 9, where the normalization constant is represented by the largest stress ratio (CB flange, stiff soil, TH7). The largest (non-normalized) stress ratio itself is well below 1. Hence, the margin with respect to the allowable limit is still significant, despite the increased seismic loads.

Similarly, the displacements of the CRDM are below the allowable limits for the deterministic analysis. The stiff soil ground configuration lead to the highest movements and also to the highest stresses for the calculated ground variabilities. The stresses at the thin lower part of the CRDM Pressure Housing are dominated through the pressure loading and the stress ratios are nearly not affected through the seismic hazard. For the upper part of the CRDM, where the movements are larger, the contribution of the seismic loading is higher. The results for the upper core plate centering pin shows also allowable stress values.

Figure 9 indicates that the stresses are not sensitive to the specific core configurations; models B, E and F lead to similar results.

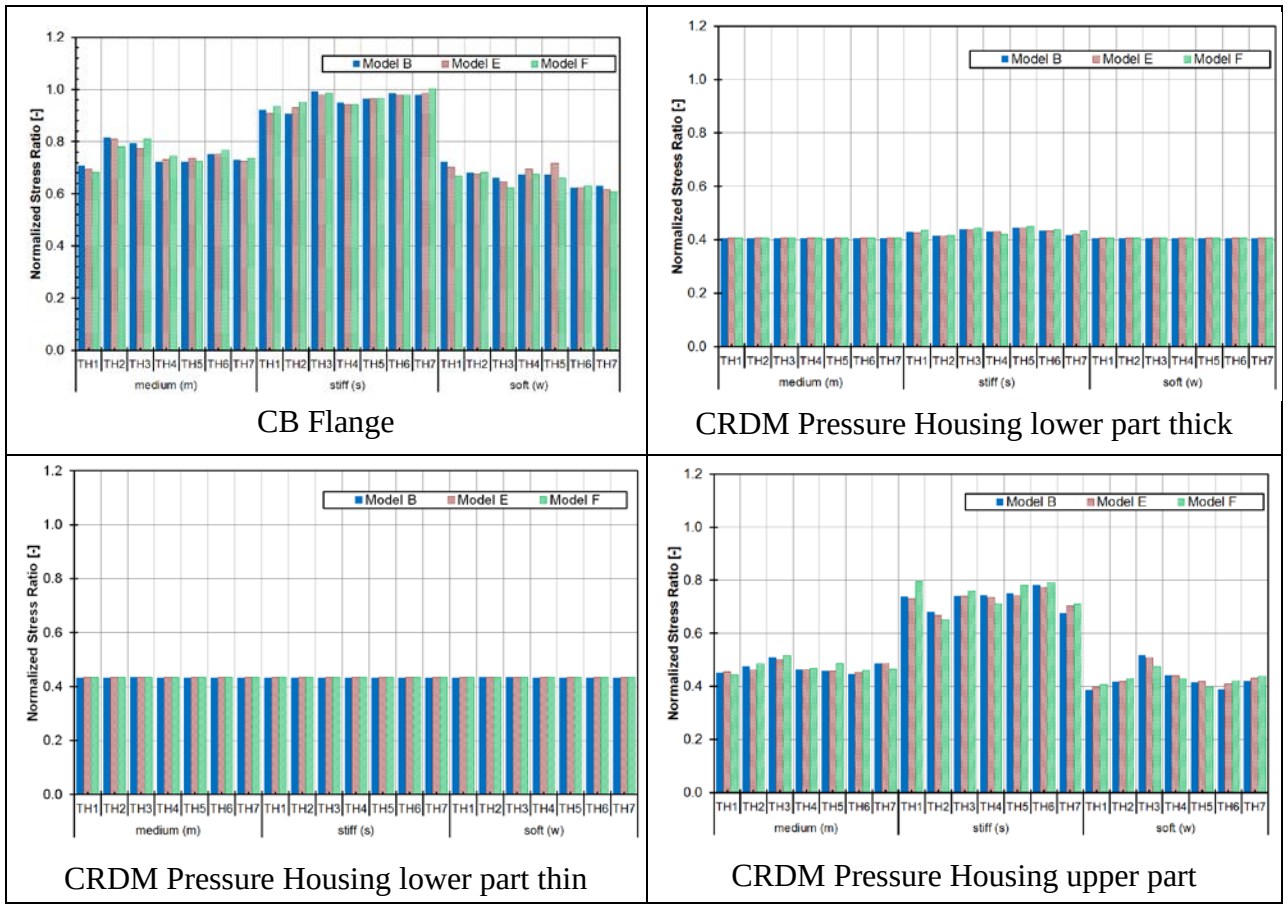

Figure 9. Normalized Stress Ratios for the core barrel (CB) flange, the CRDM Pressure housing lower part, thin and thick and upper part

For the highest stress ratios of each evaluated location of Figure 9 the distribution between seismic stress ratio and normal operation stress ratio is shown in the following figure. Again, the stress ratios are normalized by the same normalization constant. This confirms that the seismic load is of high relevance for the CB flange and the CRDM upper part, whereas the stress ratio for the CRDM lower part is mainly driven by the normal operation loading.

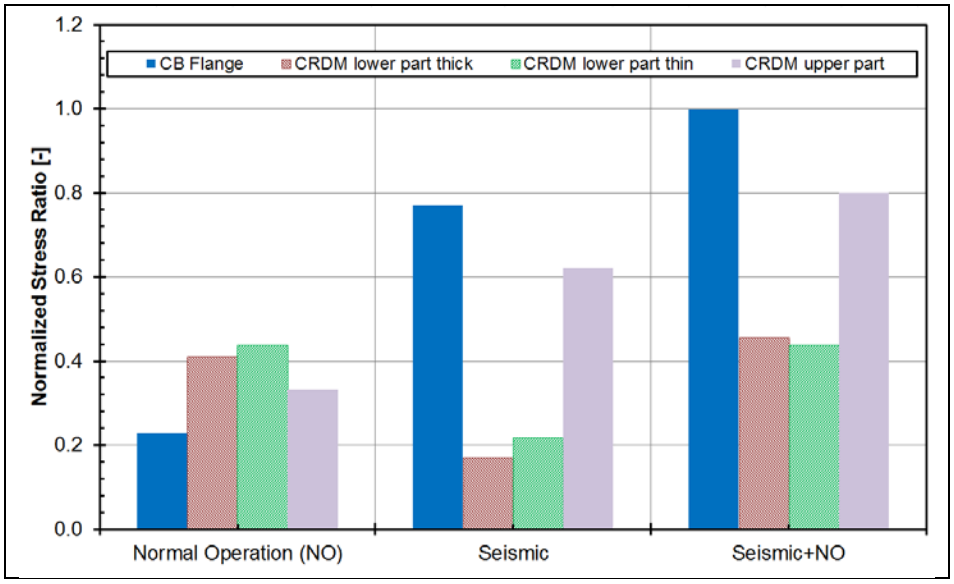

Figure 10. Contribution of normal operation (NO) and seismic loads to the final stress ratio for the most stressed parts of CB Flange and CRDM

CONCLUSIONS

The results confirm that the core barrel upper flange is the most highly stressed portions of the RPV internals.

For all evaluated parts (CB upper flange, CRDM pressure housing) the stress ratios are well below 1. Hence, the margins with respect to the allowable limits are still significant, despite the increased seismic loads.

For some time histories, a slow accumulation of relative displacement between the upper core support and upper CB flange is observed. The associated additional loads on the RPV internals are however not significant for the structural integrity of the evaluated RPV internals.

The stresses are not sensitive to the specific core configurations. The three considered core configurations (B, E and F) lead to similar results.

REFERENCES

ANSYS Release 17.2 (2016): General Purpose Finite Element Code, ANSYS Inc., Canonsburg, PA, USA

CESHOCK Version 09/89: A Spring-Lumped Mass Non-linear Dynamic Analysis Computer Code, USA

Rangelow, P. et.al. (2017). "Response of a Nuclear Power Plant Building under incoherent seismic ground motion excitation" *16th World Conference on Earthquake*, 16WCEE 2017 Santiago Chile, January 9-13, 2017.

Pellissetti, M. et.al. (2015). "Seismic robustness of reactor trip via control rod insertion at increased seismic hazard estimates" *SMiRT-23*, Manchester, UK, August 10-14, 2015. Paper ID 509